Hindawi
International Journal of Optics
Volume 2024, Article ID 5096965, 8 pages
https://doi.org/10.1155/2024/5096965

Research Article

Study on the Terahertz Spectroscopy Properties of Graphene Quantum Dots Based on Microfluidic Chip

Zhuang Peng,[1,2,3] **Yang Gao**,[1,2,3] **Xinrui Zhang**,[1,2,3] **Boyan Zhang**,[1,2,3] **Bingxin Yan**,[1,2,3] **Bo Su**,[1,2,3] **Hailin Cui**,[1,2,3] **and Cunlin Zhang**[1,2,3]

[1]*Department of Physics, Capital Normal University, Beijing 100048, China*
[2]*Key Laboratory of Terahertz Optoelectronics, Ministry of Education, Beijing 100048, China*
[3]*Beijing Key Laboratory for Terahertz Spectroscopy and Imaging, Beijing 100048, China*

Correspondence should be addressed to Bo Su; subo75@cnu.edu.cn

Received 1 December 2023; Revised 1 April 2024; Accepted 16 April 2024; Published 29 April 2024

Academic Editor: Nicola Curreli

Graphene quantum dots are quasi-zero-dimensional nanomaterials with unique physical and chemical properties. This study utilized a terahertz (THz) time-domain spectroscopy system to analyze the absorption characteristics of THz-waves by graphene quantum dots at different concentrations. Additionally, we applied electric fields and magnetic field to explore the THz-wave absorption properties of graphene quantum dots in greater detail. The results indicate that the THz absorbance of graphene quantum dots is positively correlated with sample concentration and applied electric field strength. However, it is negatively correlated with the intensity of the applied magnetic field. This work combines THz technology and microfluidic devices to propose a viable methodology for conducting in-depth study on graphene quantum dots.

1. Introduction

The term THz waves refer to electromagnetic waves whose frequency is in the range 0.1–10 THz; the wavelength that corresponds to this frequency range is 30–3000 μm [1]. The vibration and rotation modes of many biological molecules and biological molecular groups are within the THz band, and the photon energies of THz waves are low, on the order of meV, which does not damage biological molecules when used in a THz-range-based detection process. The THz time-domain spectroscopy (THz-TDS) system has a wide range of possible applications related to biological detection [2–4]. For some small biological molecules, the solid powder can be compressed to measure the fingerprint spectrum information in THz band to achieve the purpose of molecular detection. Most biological molecules can only maintain their biological activity in aqueous solutions. However, the rotational mode, vibrational mode, and energy related to hydrogen bonds between water molecules are within the THz band and will strongly absorb THz waves. In addition, water molecules are polar molecules that have strong resonance absorption to THz waves; this means it is difficult to dynamically characterize the activity of biological molecules in aqueous solutions using THz-wave-based technology [5].

Microfluidic technology permits the manipulation of very small volumes of fluid via micron-scale channels. It can reduce the propagation distance of THz waves in the fluid and thus significantly reduce the absorption of THz waves by water [6]. The combination of microfluidic devices and THz technology can reduce the consumption of samples, shorten the action distance of THz waves on samples, and permit the detection of molecules within liquid samples. Graphene quantum dots are quasi-zero-dimensional nanomaterials with numerous unique physical and chemical properties; due to the limited movement of its internal electrons in all directions, the quantum localization effect is particularly significant in graphene quantum dots [7, 8]. Graphene quantum dots have a thickness similar to that of 1–3 layers of graphene, approximately 0.4–2.0 nm. The primary difference between graphene quantum dots and graphene is in the size of plane orientation: the former is less than 100 nm, whereas

the latter is on the micron scale. Graphene quantum dots realize a transition from gapless graphene to non-zero gap graphene, which provides a basis for the fabrication of molecular graphene electronic devices.

In this study, THz technology is combined with microfluidic chip technology to study the THz absorption characteristics of graphene quantum dots in various conditions; this work presents a novel methodology for further research on graphene quantum dots. The dependence of the THz absorption of graphene quantum dots on numerous variables is studied here, including the dependence on concentration, electric field, and magnetic field.

2. Experimental Device

2.1. Experimental Optical Path. The experimental optical path is shown in Figure 1. The self-mode-locked fiber femtosecond laser independently developed by Peking University is used. Its center wavelength is 1550 nm, pulse width is 75 fs, output power is 130 mW, and pulse repetition rate is 100 MHz. The bPCA-100-05-10-1550-c-f photoconductive antenna produced by BATOP company is used to generate THz waves, the bPAC-180-05-10-1550-c-f photoconductive antenna is used to detect THz waves, and the time delay device is the electric translation platform produced by Daheng Optoelectronics Co. Ltd. The femtosecond pulse laser output by the laser is divided into two beams after passing through the polarization splitting prism. One beam, as a pump pulse, passes through the mechanical translation platform and enters the optical fiber photoconductive antenna through the optical fiber coupler to generate THz waves. Another beam, as a detection pulse, is directly coupled through the optical fiber coupler and enters the optical fiber photoconductive antenna to detect THz waves [9]. The fabricated microfluidic chip is placed in the middle of the two antennas. The THz waves generated by the THz transmitting antenna pass through the chip filled with liquid samples and carry the sample information, which is received by the detection antenna and input into the lock-in amplifier for amplification, and then the data are collected and processed by the computer.

2.2. Microfluidic Chip and Its Fabrication. The schematic diagram of microfluidic chip used in the experiment is shown in Figure 2. This microfluidic chip is simple to control, low-cost, and reusable. It is a sandwich structure, including substrate, cover, and microchannel layer. At present, the materials used to make microfluidic chips are polydimethylsiloxane (PDMS), polyethylene (PE), cyclo-olefin copolymer (COC), etc. Due to the low transmittance of PDMS to THz waves and the opacity of PE to visible light, it is impossible to observe the changes in liquid samples in the channel in real time. However, COC has high transmittance for THz waves and is less likely to react with substances. In the experiment, when the graphene quantum dot solution is injected into the microfluidic chip and left to stand for a while, it is observed that the solution does not react with COC and there is no leakage. Therefore, using

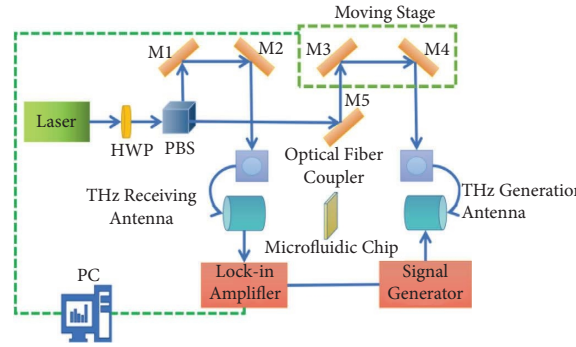

Figure 1: Experimental light path diagram.

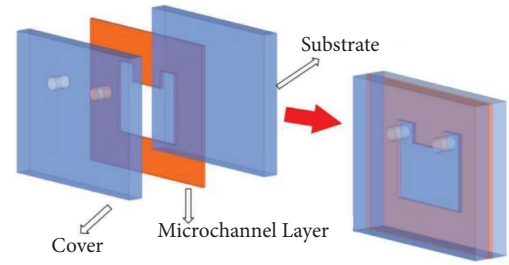

Figure 2: Schematic diagram of microfluidic chip preparation.

COC materials to make microfluidic chips is the best choice. The substrate and cover are made of COC with THz transmittance greater than 90%. A 50 μm thick strong adhesive double-sided adhesive tape is selected as the microchannel layer, and the center of the double-sided adhesive tape is hollowed out as the microchannel, which is 3 cm long and 4 cm wide. The substrate, cover, and microchannel layer are closely bonded to form a THz microfluidic chip, and the diameter of the THz detection area is 4 mm [10].

2.3. External Electric Field Device. The applied electric field device used in the experiment is shown in Figure 3. It includes sliding rheostat, switching power supply, and a high-voltage module power supply. The output of the high-voltage module power supply is, respectively, connected with two metal plates with a spacing of 4 cm. In order to ensure that the electric field of the microfluidic chip is a uniform electric field, the size of the two metal plates is much larger than that of the microfluidic chip. The microfluidic chip injected with graphene quantum dots was placed in the middle of two metal plates. The absorption characteristics of THz waves were investigated by changing the electric field intensity.

2.4. External Magnetic Field Device. The external magnetic field device used in the experiment is shown in Figure 4. A tiny electromagnet is powered by wyj-9b transistor regulated power supply to generate a magnetic field. The working voltage of the electromagnet is changed by adjusting the output voltage (output voltage range: 1–30 V) of the transistor regulated power supply, so as to adjust the strength of the magnetic field. The microfluidic chip injected with

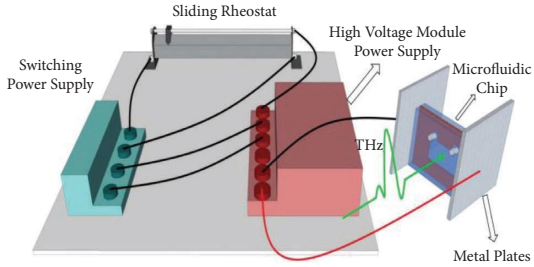

Figure 3: Schematic diagram of applied electric field device.

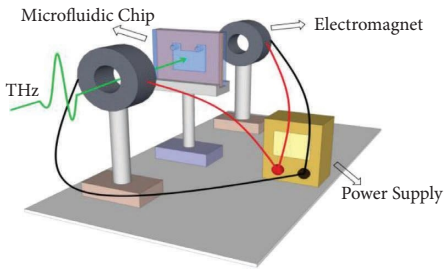

Figure 4: Schematic diagram of external magnetic field device.

graphene quantum dots was placed in the environment of different magnetic field strength, and the THz signals passing through the sample were explored through the THz time-domain spectrum system.

2.5. Configuration of Graphene Quantum Dot Aqueous Solution. The existing literature on GQDs (graphene quantum dots) is extensive. Li et al. systematically discussed the optical properties of GQDs, from mechanism, influencing factors to optical tunability [11]. Lu et al. provided the relevant characterization of graphene quantum dots, such as FTIR [12]. The GQD solution used in this study was purchased from China Suzhou Tanfeng Graphene Technology Co. Ltd. The photoluminescence quantum yield of graphene quantum dots is 9%. Graphene quantum dots emit blue light when excited by light with a wavelength in the range of 345–365 nm. Firstly, we purchased two types of GQD solutions with concentrations of 1 mg/ml and 20 mg/ml and then diluted a portion of the 20 mg/ml GQDs solution with deionized water to obtain three concentrations of 5, 10, and 15 mg/ml. Combining the initial two concentrations, we have a total of five concentrations of GQD solutions: 1, 5, 10, 15, and 20 mg/ml.

3. Experimental Methods

3.1. THz Spectral Properties of Graphene Quantum Dots at Various Concentrations. In the experiment, we selected five different concentrations of graphene quantum dots: 1, 5, 10, 15, and 20 mg/ml. The graphene quantum dots were injected into a microfluidic chip, and they were tested using a THz-TDS system to measure their time-domain spectra; the frequency-domain spectra of these graphene quantum dots were then obtained via a Fourier transform. The THz time-domain spectra and frequency-domain spectra are shown in Figures 5(a) and 5(b), respectively. In order to effectively depict the correlation between THz spectral transmittance and the concentration of graphene quantum dots at a specific frequency, we calculated the absorption coefficient at the spectral peak of 0.2 THz. As depicted in Figure 5(c), it is evident that there is an augmentation in the absorption coefficient as the concentration of the quantum dots increases. In other words, the transmittance of THz waves is negatively correlated with the concentration of graphene quantum dots. We analyzed the error of THz time-domain spectroscopy in this experiment using graphene quantum dots with a concentration of 1 mg/ml and 5 mg/ml. As shown in Figure 5(d), the difference between the 1 mg/ml and 5 mg/ml samples is greater than the data obtained after repeated measurements of 1 mg/ml. All concentration samples in this study comply with the above rules, indicating the validity of the data.

3.2. THz Spectral Properties of Graphene Quantum Dots under Different External Electric Fields. In this work, the effect of an applied electric field on graphene quantum dots was studied by controlling the intensity of the applied electric field. We used five different voltage values: 2000, 4000, 6000, 8000, and 10000 V. This corresponds to field strengths of 500, 1000, 1500, 2000, and 2500 V/cm. Each electric field strength was applied to the chip for a duration of 5 minutes. The concentration of graphene quantum dots used here is 20 mg/ml. The THz time-domain spectra and frequency-domain spectra are shown in Figures 6(a) and 6(b), respectively. Figure 6(c) shows the absorption coefficient at 0.2 THz, which increases with increasing electric field strength. In other words, the transmittance of THz waves is negatively correlated with the applied electric field intensity of the microfluidic chip. Figure 6(d) shows the THz time-domain spectra of graphene quantum dots under electric field intensities of 0.5 kV/m and 1 kV/m. It can be seen that the difference in THz time-domain signal strength of the sample under the action of 0.5 kV/m and 1 kV/m electric fields is greater than the signal strength measured twice under the action of 0.5 kV/m electric fields. Due to the fact that all samples under the electric field intensity comply with the above rules, it indicates the validity of the data.

3.3. THz Spectral Properties of Graphene Quantum Dots under External Magnetic Field. The influence of a magnetic field on graphene quantum dots is studied here by controlling the external magnetic field magnitude. The applied magnetic field strength is varied by changing the output voltage of the regulated power supply (six output voltage values of 0, 3, 6, 9, 12, and 15 V were used, i.e., magnetic field strengths of 0, 6, 12, 18, 24, and 30 mT), and the chip was subject to this field for 5 min. The concentration of graphene quantum dots used here is 20 mg/ml. The THz time-domain spectra are shown in Figure 7(a), and the THz frequency-

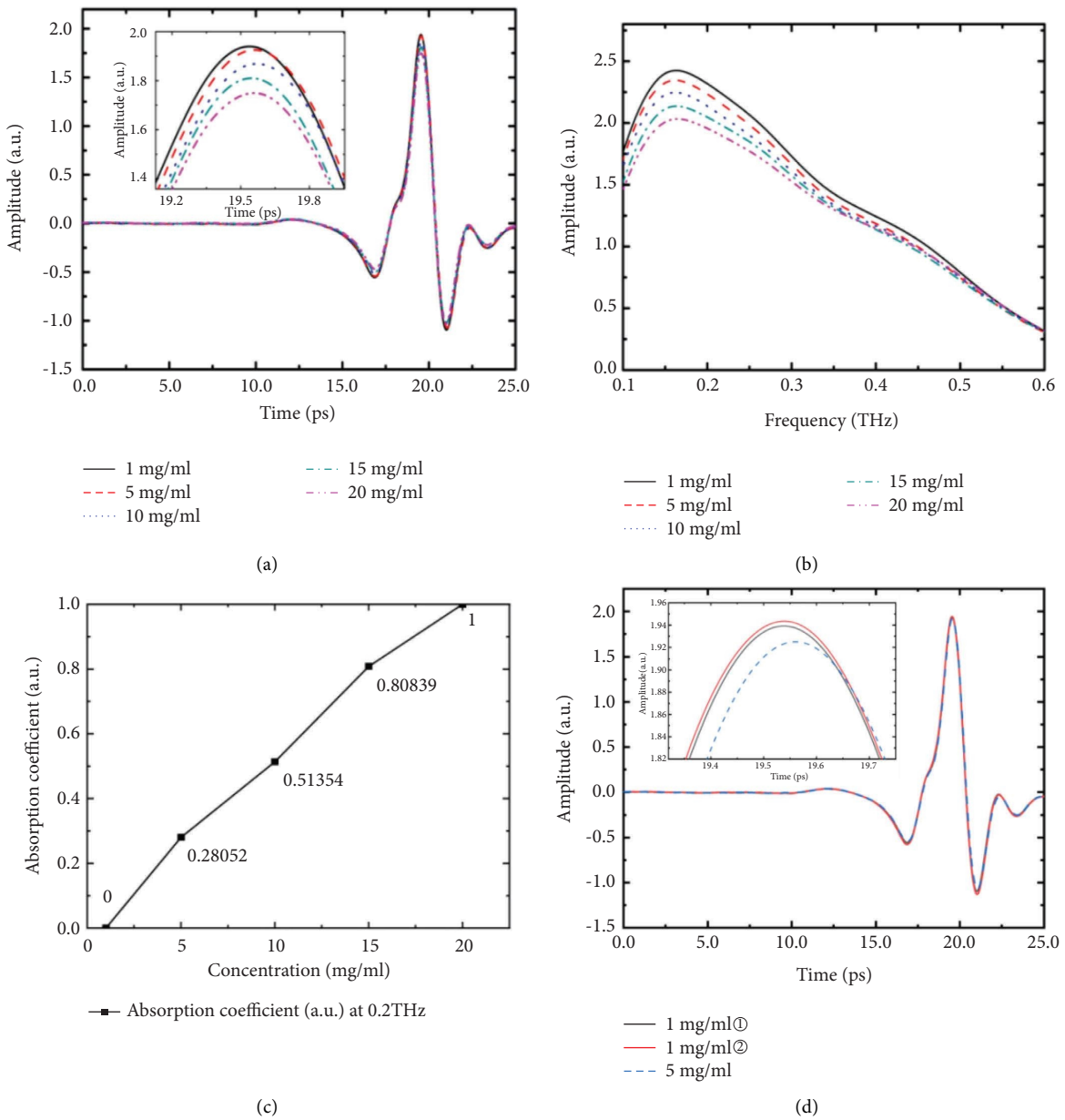

Figure 5: (a) THz time-domain spectra at various concentrations of graphene quantum dots. (b) Frequency-domain spectra at various concentrations of graphene quantum dots. (c) Absorption coefficient at various concentrations of graphene quantum dots at 0.2 THz. (d) THz time-domain spectra of 1 mg/ml and 5 mg/ml graphene quantum dots.

domain spectra are shown in Figure 7(b). Figure 7(c) shows the absorption coefficient at 0.2 THz, which decreases with increasing magnetic field strength. It can be seen that the transmittance of THz waves is positively correlated with the applied magnetic field intensity of the microfluidic chip. Figure 7(d) shows the THz time-domain spectra of graphene quantum dots under magnetic field intensities of 0 mT and 6 mT. It can be seen that the difference in THz time-domain signal strength of the sample under the action of 0 mT and 6 mT magnetic fields is greater than the signal strength measured twice under the action of 0 mT magnetic fields. All samples under magnetic field intensity comply with the above rules, and the data are valid.

4. Result and Discussion

The method used in this study to calculate the absorption coefficient is similar to Liu et al. [13], and the calculation formula is as follows:

$$n = 1 + \frac{c}{\omega d}\phi(\omega),$$
$$\alpha = -\frac{2}{d}\ln\left[\frac{(n+1)^2}{4n}\left|\frac{E_{\text{sample}}}{E_{\text{reference}}}\right|\right]. \quad (1)$$

In the formula, n represents the refractive index of the sample, c is the speed of light, ω is the angular frequency of

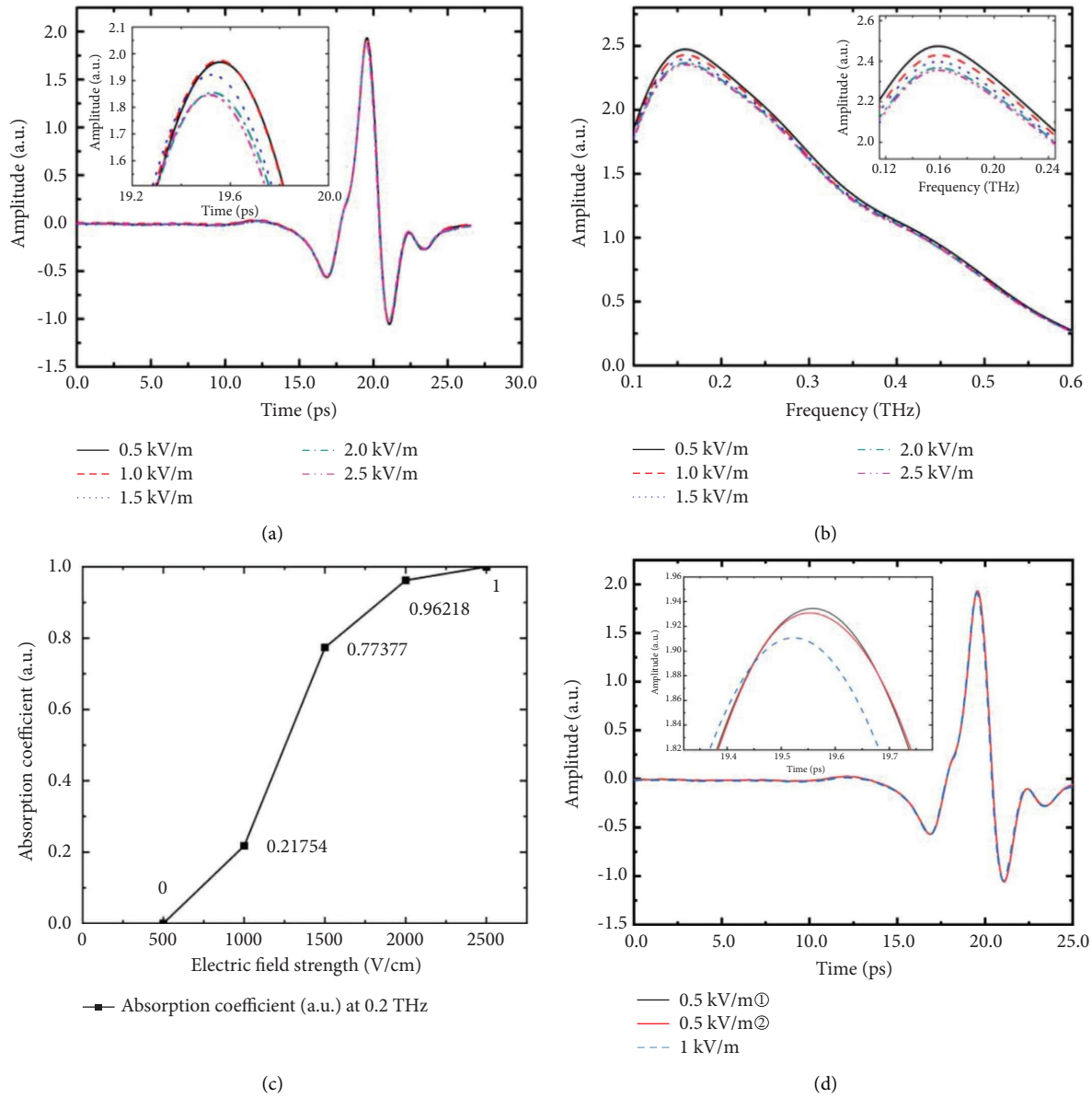

Figure 6: (a) THz time-domain spectra under different electric field strengths. (b) Frequency-domain spectra under different electric field strengths. (c) Absorption coefficient under different electric field strengths at 0.2 THz. (d) THz time-domain spectra of graphene quantum dots under electric field intensities of 0.5 kV/m and 1 kV/m.

the THz wave, d is the sample thickness, and $\phi(\omega)$ is the phase difference between the sample signal and the reference signal. E_{sample} and $E_{\text{reference}}$ are the amplitudes of the sample and reference signals, respectively, and α is the absorption coefficient. Figures 5(c), 6(c), and 7(c) normalize the original data to better observe linear trends and elucidate the relationship between absorption coefficient and concentration, electric field strength, and magnetic field strength.

Figure 5 illustrates the relationship between the concentration of graphene quantum dots and the transmission of the THz spectrum. It reveals that the transmittance of THz waves is negatively correlated with the concentration of graphene quantum dots. In other words, higher concentrations of graphene quantum dots result in a stronger absorption of THz waves. Figure 8 depicts the structure of graphene quantum dots bearing hydroxyl and carboxyl functional groups. The existence of these functional groups renders the graphene quantum dots more unstable than regular graphene. Both hydroxyl and carboxyl groups readily form hydrogen bonds with water molecules [14]. Intermolecular hydrogen bonds are highly sensitive to THz waves and display strong absorption [15]. As the concentration of the graphene quantum dot solution increases, more graphene quantum dots bind to water molecules, leading to heightened absorption of THz waves.

Figure 6 shows that the transmittance of THz waves is negatively correlated with the applied electric field intensity of the microfluidic chip. In other words, the stronger the

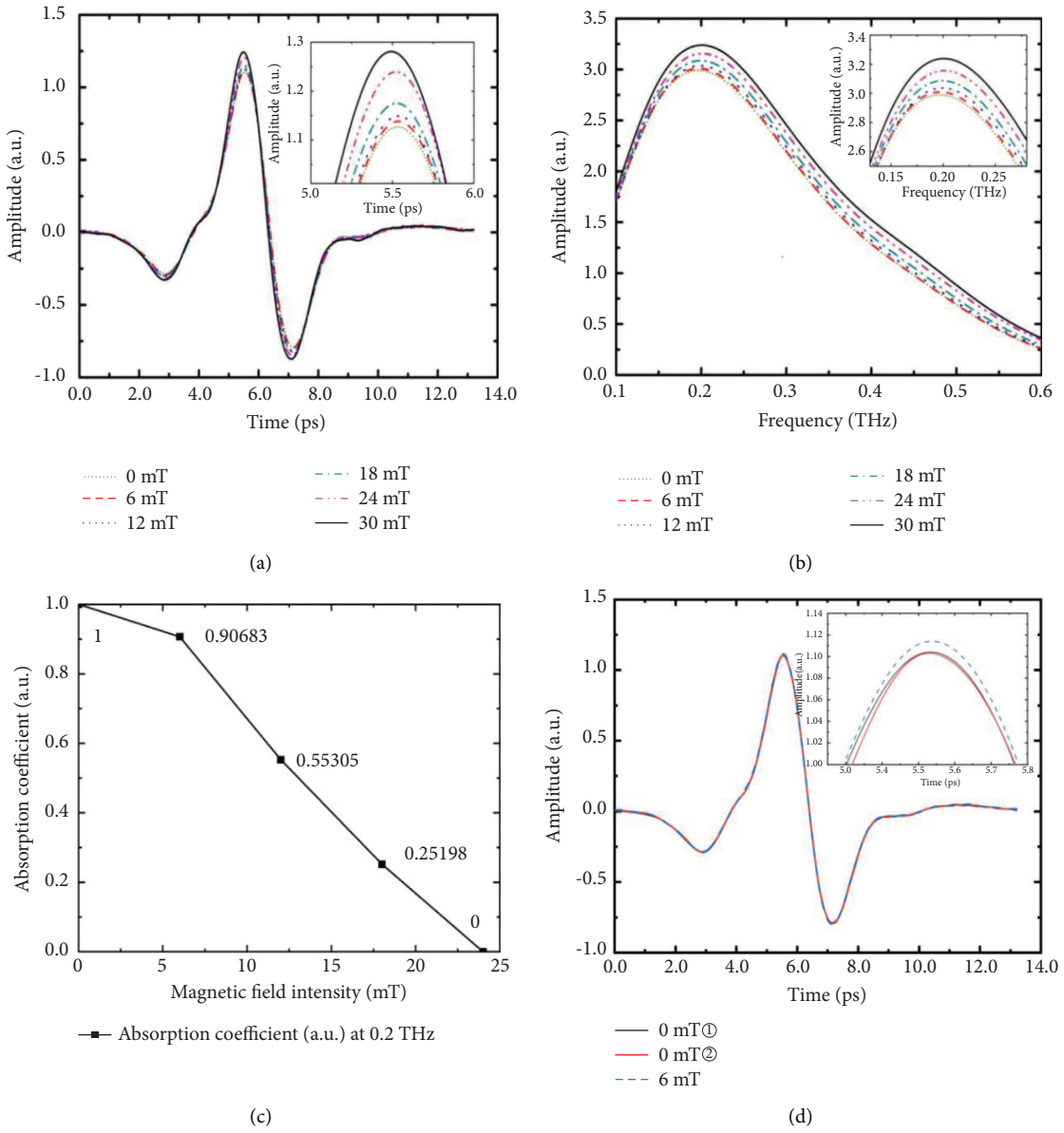

Figure 7: (a) THz time-domain spectra under different magnetic field strengths. (b) Frequency-domain spectra under different magnetic field strengths. (c) Absorption coefficient under different magnetic field strengths at 0.2 THz. (d) THz time-domain spectra of graphene quantum dots under magnetic field intensities of 0 mT and 6 mT.

applied electric field intensity, the stronger the absorption of THz waves by graphene quantum dots. In addition, under a given electric field intensity, the absorption of THz waves by graphene quantum dots gradually increases with the increase in the duration for which the sample is subject to the electric field. When $\pi D/\lambda < 0.3$, Rayleigh scattering is the primary factor that affects the transmittance of THz radiation [16]. Yan investigated the influence of particle size on THz spectral scattering using the Rayleigh scattering formula [17]. At a certain scattering angle, the scattering intensity of the scattered light with the particles separated by a distance of r:

$$I = \frac{\pi^4 d^6}{8\lambda^4 r^2}\left(\frac{n^2-1}{n^2+2}\right)^2\left(1+\cos^2\theta\right)I_0, \tag{2}$$

where d represents particle size, λ denotes the incident light wavelength, and n stands for the refractive index of the particles. The intensity of scattered light is proportional to the sixth power of the particle size. Due to the relatively large particle size of graphene quantum dots, they exhibit electrophoresis phenomenon in an electric field, leading to particle aggregation and increased particle size. This results in enhanced Rayleigh scattering of THz waves. With an

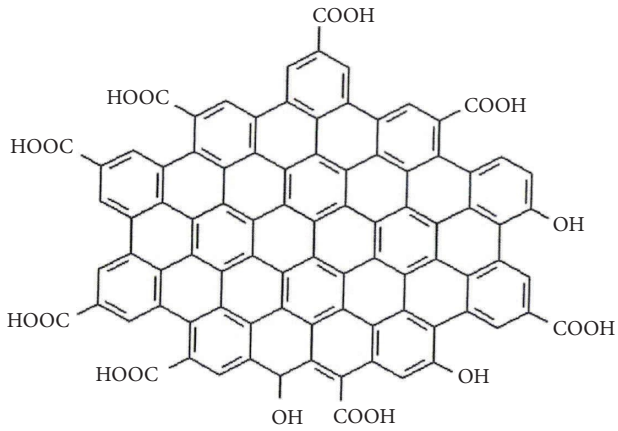

Figure 8: Schematic diagram of graphene quantum dots.

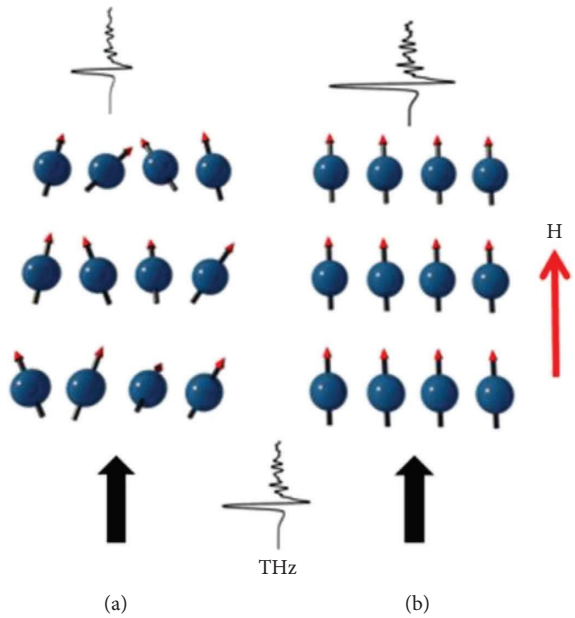

Figure 9: Under the applied magnetic field, the arrangement of particles and their influence on the THz propagation. (a) Graphene quantum dots are randomly oriented and THz undergoes isotropic absorption. (b) The particles align along the direction of the applied magnetic field. The applied magnetic field direction is orthogonal to the THz polarization direction. The absorption rate of THz decreases.

increase in electric field intensity, more graphene quantum dots undergo particle aggregation, further increasing the particle size and scattering intensity, consequently reducing the transmittance of THz waves.

Shalaby et al. utilized THz technology to investigate ferrofluids subjected to a magnetic field [18]. When the magnetic field is orthogonal to the polarization direction of the THz wave, the absorption of THz by the ferrofluid decreases as the magnetic field intensity increases. In this study, graphene quantum dots were prepared using a chemical method, containing chemical groups such as hydroxyl, resulting in the generation of magnetic moments on the surface defects [19]. Graphene quantum dots exhibit similar properties to ferrofluids under a magnetic field, where particles tend to align along the magnetic field direction. As the magnetic field intensity increases, a decrease in THz absorption is also observed. In the absence of an external magnetic field, the particles are randomly oriented, resulting in zero net magnetic orientation (Figure 9(a)). In this case, the THz wave undergoes isotropic absorption. In the presence of an external magnetic field, the particles tend to align along the direction of the magnetic field (Figure 9(b)). In this case, the THz wave undergoes anisotropic absorption, and the absorption rate decreases with increasing magnetic field strength when the direction of the magnetic field is perpendicular to the polarization direction of the THz wave.

5. Conclusion

This study combines THz time-domain spectroscopy with microfluidic chip technology to detect graphene quantum dots of different concentrations. The research reveals that as the concentration of graphene quantum dots increases, the hydrogen bond content in the solution increases, leading to a stronger absorption of THz waves by the graphene quantum dots and a lower transmittance of THz waves. Applying an electric field on the microfluidic chip causes particle aggregation of graphene quantum dots, enhancing the Rayleigh scattering. The greater the electric field intensity, the lower the transmittance of THz waves. When a magnetic field is applied to a microfluidic chip, graphene quantum dot particles align in the direction of the magnetic field. When the direction of the magnetic field is orthogonal to the polarization direction of the THz wave, the absorption rate decreases as the strength of the magnetic field increases. That is, the stronger the magnetic field, the higher the transmission rate of the THz wave. Future work should focus on utilizing the THz absorption characteristics of graphene quantum dots to study their applications in the THz field.

Data Availability

Data underlying the results presented in this paper are not publicly available at the time of publication but may be obtained from the authors upon reasonable request.

Conflicts of Interest

The authors declare that they have no conflicts of interest.

Acknowledgments

The authors would like to express their gratitude to EditSprings (https://www.editsprings.cn) for the expert linguistic services provided. This work was funded by the National Key R&D Program of China (grant no. 2021YFB3200100), National Natural Science Foundation of China (NSFC) (61575131), and Beijing Municipal Natural Science Foundation (4232066).

References

[1] Z. Li, B. Jiao, W. Liu et al., "High-efficiency terahertz wave generation with multiple frequencies by optimized cascaded difference frequency generation," *Chinese Physics B*, vol. 30, no. 4, Article ID 44211, 2021.

[2] J. Fang, Z. Zhang, Y. Bo et al., "Vibrational spectral and structural characterization of multicomponent ternary co-crystal formation within acetazolamide, nicotinamide and 2-pyridone," *Spectrochimica Acta Part A: Molecular and Biomolecular Spectroscopy*, vol. 245, Article ID 118885, 2021.

[3] Y. Du, Y. Wang, J. Xue, J. Liu, J. Qin, and Z. Hong, "Structural insights into anhydrous and monohydrated forms of 2,4,6-trihydroxybenzoic acid based on Raman and terahertz spectroscopic characterization," *Spectrochimica Acta Part A: Molecular and Biomolecular Spectroscopy*, vol. 224, Article ID 117436, 2020.

[4] A. Gong, Y. Qiu, X. Chen, Z. Zhao, L. Xia, and Y. Shao, "Biomedical applications of terahertz technology," *Applied Spectroscopy Reviews*, vol. 55, no. 5, pp. 418–438, 2019.

[5] Y. Cai, J. Wang, Z. Bai et al., "Terahertz transmission characteristics of water induced by electric field," *Spectroscopy and Spectral Analysis*, vol. 41, p. 1683, 2021.

[6] N. Fan, B. Su, Y. Wu et al., "Sandwich terahertz microfluidic chip," *Spectroscopy and Spectral Analysis*, vol. 38, no. 05, pp. 1362–1367, 2018.

[7] A. D. Güçlü, P. Potasz, M. Korkusinski, and P. Hawrylak, "Graphene quantum dots," *NanoScience and Technology*, vol. 31, pp. 415–428, 2014.

[8] H. Sun, L. Wu, W. Wei, and X. Qu, "Recent advances in graphene quantum dots for sensing," *Materials Today*, vol. 16, no. 11, pp. 433–442, 2013.

[9] Y. Wu, B. Su, J. He, and C. Zhang, "Terahertz absorption properties of electrolyte solutions based on microfluidic chip," *Spectroscopy and Spectral Analysis*, vol. 39, pp. 2348–2353, 2018.

[10] B. Su, C. Zhang, N. Fan, and C. Zhang, "Terahertz microfluidic chips for detection of amino acids in aqueous solutions," *Heliyon*, vol. 8, 2016.

[11] L. Li, G. Wu, G. Yang, J. Peng, J. Zhao, and J.-J. Zhu, "Focusing on luminescent graphene quantum dots: current status and future perspectives," *Nanoscale*, vol. 5, no. 10, pp. 4015–4039, 2013.

[12] Lu Rui-rui, L. Yi-si, L. Peng, and C. Xiao-juan, "Preparation, characterization and application of graphene quantum dots," *Carbon Techniques*, vol. 33, no. 03, pp. 1–5, 2014.

[13] Q. Liu, D. Luo, X. Zhang, S. Li, and Z. Tian, "Refractive index and absorption coefficient of blue phase liquid crystal in terahertz band," *Liquid Crystals Reviews*, vol. 44, pp. 348–354, 2017.

[14] P. Taday, "Applications of terahertz spectroscopy to pharmaceutical sciences," *Philosophical Transactions of the Royal Society of London,Series A: Mathematical, Physical and Engineering Sciences*, vol. 362, no. 1815, pp. 351–364, 2004.

[15] Y. Wu, B. Su, J. He, and C. Zhang, "Study on terahertz absorption characteristics of electrolyte solution based on microfluidic chip," *Spectroscopy and Spectral Analysis*, vol. 39, no. 08, pp. 2348–2353, 2019.

[16] N. Mingo, K. Esfarjani, D. Broido, and D. A. Stewart, "Cluster scattering effects on phonon conduction in graphene," *Physical Review B: Condensed Matter*, vol. 81, no. 4, Article ID 045408, 2010.

[17] F. Yan, *Study on Sample Scattering in Terahertz Time Domain Spectroscopy*, Ph.D. dissertation, University of Science and Technology Beijing, Beijing, China, 2016.

[18] M. Shalaby, M. Peccianti, Y. Ozturk, I. Al-Naib, C. P. Hauri, and R. Morandotti, "Terahertz magnetic modulator based on magnetically clustered nanoparticles," *Applied Physics Letters*, vol. 105, no. 15, Article ID 151108, 2014.

[19] Y. Sun, Y. Zheng, H. Pan et al., "Magnetism of graphene quantum dots," *NPJ Quantum Materials*, vol. 2, no. 1, 2017.